

c.1

LOAN COPY: RETUR
Commander
Air Force Special Weapons C
ATTN: Tech Info & Intel Ofi
Kirtland AFB, New Mexico

0152717

TECH LIBRARY KAFB, NM



TECHNICAL NOTE

D-II

MEASURED AND PREDICTED SECTION WAVE DRAG COEFFICIENTS
AT A MACH NUMBER OF 1.6 FOR A DELTA WING
WITH TWO AIRFOIL SECTIONS

By Frederick C. Grant

Langley Research Center
Langley Field, Va.

NATIONAL AERONAUTICS AND SPACE ADMINISTRATION
WASHINGTON

September 1959



0152717

NATIONAL AERONAUTICS AND SPACE ADMINISTRATION

TECHNICAL NOTE D-11

MEASURED AND PREDICTED SECTION WAVE DRAG COEFFICIENTS

AT A MACH NUMBER OF 1.6 FOR A DELTA WING

WITH TWO AIRFOIL SECTIONS

By Frederick C. Grant

SUMMARY

Experimental and theoretical section wave drag coefficients for a 60° delta wing with two airfoil sections are presented for a Mach number of 1.6. One airfoil section was an NACA 65A006, and the other was that 6-percent section which gives a delta wing the longitudinal cross-sectional area distribution of a Sears-Haack optimum body of revolution for a given length and volume.

For a given airfoil section the experimental chordwise pressure distributions were much the same at every spanwise station. Hence, the results showed only small measured variations of section wave drag coefficient along the span in contrast to the larger variations predicted by linear theory.

The experimental spanwise drag loadings were nearly the same for the two airfoil sections. The 65A wing had about three-fourths of the wave drag coefficient of the Sears-Haack wing. The linear theory did predict the 65A section to be the better section at a Mach number of 1.6, but made a 17-percent error in the amount of the drag of this section.

INTRODUCTION

The section wave drag coefficient is not usually constant along the span of a wing and is sometimes subject to large variations. (See refs. 1 and 2.) Experimental variations of wing-section wave drag are needed to evaluate the accuracy of the linear theory. This paper will give a comparison of the theoretical and experimental section wave drag for two airfoil sections on a delta plan form. One airfoil section is such that the cross-sectional area distribution of the wing is that of a Sears-Haack optimum body of given length and volume. (See ref. 3.) The other airfoil is a standard 65A section. (See ref. 4.) The thickness ratio is 6 percent for both wings; thus, the wing volumes are not equal.

Polygonal approximations to the actual airfoil sections will be used in the theory. It is recognized that this assumption leads to infinite discontinuities in the linearized pressure distribution for ridge lines swept behind the Mach lines. Approaches treating the nose as actually blunt, such as those of reference 5, are needed to obtain realistic pressure distributions. Such a refinement in detail cannot be expected to influence greatly the spanwise variation of the integrated pressure distributions calculated for a polygonal simulation of an actual airfoil. Such spanwise variations are the principal concern of this paper.

SYMBOLS

A	cross-sectional area
b	wing span
B	cotangent of Mach angle
c	wing chord
\bar{c}	average chord
c_d	section wave drag coefficient
c_n	section normal-force coefficient
C_D	wave drag coefficient of wing
C_L	lift coefficient
C_N	wing normal-force coefficient
C_p	pressure coefficient on wing, $\frac{p - p_\infty}{q}$
l	wing length in stream direction
m	tangent of semiapex angle of delta wing
M	Mach number
n	tangent of Mach angle divided by tangent of wing semiapex angle

N	number of sides of polygonal airfoil
p	pressure
p,a,b	summation limits
q	dynamic pressure
R	Reynolds number
t	maximum thickness of wing section
t_r	thickness ratio of polygonal airfoil
$t_{\alpha\beta}$	β times the slope of a line from the apex of wing α to leading edge of wing β at station η ($t_{\alpha\beta} = 0$ for $\eta = 0$)
x,y,z	Cartesian coordinates
x_i	chordwise position of the i th corner of polygonal airfoil
z	height of surface from chord plane on test model
z_i	height of i th corner of polygonal airfoil
α, β, i	indices
η	spanwise station, fraction of semispan, $\eta = 0$ on root chord
$\Delta\lambda$	slope change at corners of polygonal airfoil
λ_i	slope of i th side of polygonal airfoil
$l - \mu$	root chord of arrow wing
ρ, σ, τ, v	streamwise line integrals of pressure coefficients

Subscripts:

t	tip
∞	free-stream

MODELS

The two steel semispan test models had the delta plan form shown in figure 1. The airfoil section and thickness ratio were constant along the span of each model. Based on the streamwise length of the models, the thickness ratio at the root was 6 percent. Orifices were placed in streamwise rows at five spanwise stations which are marked in figure 1 at the leading edge of the wing in $\frac{2y}{b}$ units.

The root sections of the two test models are shown in figure 2. The section labeled Sears-Haack is derived in reference 6 from the Sears-Haack body of minimum drag for a given length and volume. A constant-thickness-ratio delta wing with what is called, for convenience, a Sears-Haack section has the cross-sectional area distribution of a Sears-Haack body of minimum drag for given length and volume. The wing with the Sears-Haack section is called, for convenience, a Sears-Haack wing. On the test Sears-Haack wing the metal became too thin for machining near the trailing edge and the delta wing was cut off at 90 percent of the chord. Consequently, the rear 10 percent of the length of the truncated model has the cross-sectional area distribution of a cone rather than that of a Sears-Haack body. The other curve shown in figure 2 is a standard NACA 65A thickness distribution.

The cross-sectional area distributions of the two models are shown in figure 3. This figure shows that the 65A wing has more volume and a lower effective fineness ratio than does the Sears-Haack wing. These fineness ratios are 6.2 for the Sears-Haack wing and 5.4 for the 65A wing.

TESTS

The models were mounted on a boundary-layer bypass plate and were tested in the Langley 4- by 4-foot supersonic pressure tunnel, a closed return pressurized tunnel, which is described in reference 7. Pressure measurements were obtained with and without fixed transition near the leading edge. Two tunnel pressures were used to give Reynolds numbers of 2.0×10^6 and 4.3×10^6 based on the mean aerodynamic chord of the full-delta plan form. Data were taken at angles of attack up to 14° . The angles were set manually with the aid of a divided circle.

PRESSURE DISTRIBUTIONS

For all the pressure distributions to follow, the Reynolds number of 4.3×10^6 was based on the mean aerodynamic chord of the full-delta wing. Transition is fixed unless otherwise noted. No significant effects of Reynolds number were observed. The pressure-coefficient data are given in tables I and II for the whole range of angles of attack and test conditions.

Pressures at Zero Lift

Normal to chord.- The chordwise pressure distributions over the wing sections at the five spanwise stations are shown in figure 4 for the attitude of zero lift and circulation at $\alpha = 0^\circ$. The most distinctive feature of these plots is the small change in the distributions with spanwise station, particularly for the 65A section. Generally speaking, the pressure variation is much more smooth and gradual on the chord of the 65A wing. Higher negative peak pressures exist on the Sears-Haack wing.

Parallel to chord.- The pressure distributions at $\alpha = 0^\circ$ are plotted against surface height in figure 5. Pressure values for one surface of the wing are shown for two boundary-layer conditions: a low Reynolds number natural-transition case, and a higher Reynolds number fixed-transition case. The area of the loop on either side of the $\frac{2z}{t} = 0$ line is proportional to the section drag coefficient in each case. It is plain that the influence on the section drag of fixed transition at the higher Reynolds number is rather slight. The high negative pressure peaks observed on the Sears-Haack wing in figure 4 are seen to contribute to higher drag coefficients on the Sears-Haack wing since the peaks occur behind the maximum thickness point. The higher positive pressures near the nose of the Sears-Haack wing also indicate higher drags on the Sears-Haack wing. These higher pressures near the nose can be attributed to the larger nose radius of the Sears-Haack section which is apparent in figure 2.

Pressures at Positive Lift

The chordwise pressure distributions are shown in figure 6 for angles of attack of 4° and 8° . The pressure peak characteristic of thin lifting sweptback wings at supersonic speeds may be observed near the inboard leading edge of the low-pressure surfaces at $\alpha = 8^\circ$. It can be seen to spread in the chordwise direction at the more outboard

stations. At the most outboard station $\frac{2y}{b} = 0.80$, the flow on the low-pressure surfaces appears to be separated.

INTEGRATED PRESSURES

Zero Lift Conditions

Experimental section wave drag coefficients along the span and experimental spanwise wave drag distributions are shown in figure 7. Corresponding values computed by the linearized theory technique outlined in the appendix are shown for comparison. For theoretical computations the Sears-Haack wing was considered to be a complete delta wing. It is interesting to note in figure 7(a) that the large spanwise gradients in section drag coefficient predicted by linear theory for the Sears-Haack section shape do not appear. In fact, there is little spanwise change in actual section drag coefficient and nearly a constant difference in section drag coefficient between airfoils. This similarity in section drag coefficient distribution along the span is reflected in practically identical normalized spanwise drag distributions as shown in figure 7(b). The increments between airfoils indicated by the theory do not appear.

To the right of figure 7(a) the values of C_D according to the experiment and theory are marked on the same scale as C_d . The relative merit of the two wings is predicted correctly, but the magnitudes of the drags are not predicted correctly by the theory. The 65A section is much better than was predicted. The close agreement of the measured and predicted values of C_D for the Sears-Haack section must be regarded as fortuitous.

Experimentally, the 65A wing has the lower drag. Qualitatively then, it seems that there is a contradiction since the Sears-Haack wing is supposedly equivalent to a body of minimum drag for a given length and volume. It must be remembered, however, that, although a Sears-Haack body may be an optimum body for $M = 1$ (as shown in reference 8 it is not, strictly speaking, an optimum body), it is not necessarily one at $M = 1.6$. In fact, if the optimum polygonal airfoil section for a delta wing of a given length and volume at $M = 1.66$ (ref. 6) is compared with the polygonal approximation of a 65A section as in figure 8, a close resemblance may be seen. The contradiction, then, is only apparent and superficial.

Lifting Conditions

Corresponding to the pressures at a positive lift plotted in figure 6, the integrated force coefficients are shown in figure 9. Additional data at angles of attack of 2° and 6° are included.

Figure 9 indicates no significant influence of section shape on the span loading or normal forces. Linearized-theory predictions of these quantities are shown for comparison.

CONCLUDING REMARKS

Small experimental spanwise variations of section wave drag coefficient for both wings occurred. Larger spanwise variations were predicted by linear theory for the Sears-Haack wing. The small spanwise variations of section wave drag coefficient indicate that, for many cases, a strip theory of wing-wave-drag prediction would give accurate results if a good value of section wave drag coefficient could be estimated. Linear-theory predictions of section drag coefficients are obviously inadequate, in general.

The experimental spanwise drag loadings were nearly identical for the two airfoil sections. Linear theory correctly predicted the better airfoil section at a Mach number of 1.6 but gave a 17-percent error in the amount of the drag of the 65A wing. The 65A wing had a wave drag coefficient that was about three-fourths of that for the Sears-Haack wing.

Langley Research Center,
National Aeronautics and Space Administration,
Langley Field, Va., March 6, 1959.

APPENDIX

CALCULATION OF SECTION DRAG COEFFICIENTS

General Considerations

Consider a delta wing of unit root chord and semispan m . (See fig. 10.) The wave drag of such wings at zero angle of attack with N -sided polygonal airfoil sections is calculated by the methods of linear theory in references 6 and 9. If an integration in the streamwise direction is substituted for the integration over the wing area, which is performed in reference 9, a section drag coefficient may be obtained in the following form:

$$\frac{\pi}{8m} \left\{ \frac{cc_d}{t_r^2} \right\} = \sum_{\alpha=2}^p \sum_{\beta=1}^{\alpha-1} \rho_{\alpha\beta} \Delta\lambda_\alpha \Delta\lambda_\beta + \sum_{\alpha=1}^p \sum_{\beta=1}^N \sigma_{\alpha\beta} \Delta\lambda_\alpha \Delta\lambda_\beta + \sum_{\alpha=p+1}^N \sum_{\beta=1}^b \tau_{\alpha\beta} \Delta\lambda_\alpha \Delta\lambda_\beta + \sum_{\alpha=p+1}^a \sum_{\beta=1}^N v_{\alpha\beta} \Delta\lambda_\alpha \Delta\lambda_\beta \quad (A1)$$

The separate terms of this summation may each be regarded as the section wave drag of a wing β that is due to a wing α . Wings α and β are wedge-section delta wings of wedge semiangle $\Delta\lambda_\alpha$ and $\Delta\lambda_\beta$, respectively. The apexes of wing α and wing β are at the α and β division points of the delta-wing root chord, if the leading edge is given the number 1. (See fig. 10.) The functions ρ and σ are applicable to wings α with subsonic leading edges; ρ applies to the region between the Mach line and leading edge and σ applies to the region behind the leading edge of wing α . For $\alpha > p$, wings α have supersonic leading edges and functions τ and v are applicable. The function τ applies to the region between the leading edge and Mach line; v applies to the region behind the Mach line of wings α . Combinations of α and β for which there is no interaction are eliminated by restricting $\alpha \leq a$ and $\beta \leq b$ in the τ and v summations. The $\Delta\lambda$ values are proportional to the changes in slope at the corners of the delta-wing polygonal airfoil. The $\Delta\lambda$ values are defined as follows:

$$\left. \begin{aligned} \lambda_0 &= 0 \\ \Delta\lambda_i &= \lambda_i - \lambda_{i-1} \\ \lambda_i &= \frac{z_{i+1} - z_i}{t_r(x_{i+1} - x_i)} \end{aligned} \right\} \quad (A2)$$

The t_r parameter in formulas (A1) and (A2) represents the thickness ratio of the polygonal section. Special restrictions of $\Delta\lambda$ are implied by the conditions that there is no downwash behind the trailing edge and that the airfoil thickness is zero at the trailing edge. These conditions, respectively, imply that for no downwash

$$\sum_{\beta=1}^{N+1} \Delta\lambda_{\beta} = 0 \quad (A3a)$$

and for a sharp trailing edge

$$\sum_{\beta=1}^{N+1} \beta \Delta\lambda_{\beta} = 0 \quad (A3b)$$

The p , a , and b limits of the summations in equation (A1) are the largest integers satisfying the inequalities

$$\left. \begin{aligned} p &< l + N(l - Bm) \\ a &< (N + 1)(l - \eta) + \eta[l + N(l - Bm)] \\ b &< \frac{\alpha - \eta[l + N(l - Bm)]}{1 - \eta} \\ p &\leq N \quad a \leq N \quad b \leq N \end{aligned} \right\} \quad (A4)$$

The symbol N represents the number of sides of the polygonal airfoil; $\eta = \frac{y}{m}$ defines the spanwise station; and $B = \sqrt{M^2 - 1}$ is the cotangent of the Mach angle.

The ρ function is defined by the formula

$$\rho_{\alpha\beta} = \frac{n_\alpha}{\sqrt{n_\alpha^2 - 1}} \left(\eta \left(\log_e n_\alpha - \frac{1}{t_{\alpha\beta}} \cosh^{-1} \sqrt{\frac{n_\alpha^2 - 1}{t_{\alpha\beta}^2 - 1}} + \right. \right. \\ \left. \left. \frac{1}{2} \eta \log_e \frac{\sqrt{n_\alpha^2 - t_{\alpha\beta}^2} + t_{\alpha\beta} \sqrt{n_\alpha^2 - 1}}{t_{\alpha\beta} \sqrt{n_\alpha^2 - 1} - \sqrt{n_\alpha^2 - t_{\alpha\beta}^2}} \right) \quad (n_\alpha > t_{\alpha\beta} > 1) \right) \quad (A5a)$$

Formula (A5a) may be used when $t_{\alpha\beta}$ is outside the specified range of definition if a special argument $t'_{\alpha\beta}$ is substituted for $t_{\alpha\beta}$ as follows:

$$\left. \begin{array}{ll} t'_{\alpha\beta} = n_\alpha & (t_{\alpha\beta} > n_\alpha; t_{\alpha\beta} < 0) \\ t'_{\alpha\beta} = 1 & (1 > t_{\alpha\beta} > 0) \end{array} \right\} \quad (A5b)$$

A special value of ρ is

$$\rho_{\alpha\beta} = 0 \quad (t_{\alpha\beta} = 1) \quad (A5c)$$

Corresponding formulas for σ are for $n_\alpha > 1 > t > 0$

$$\sigma_{\alpha\beta} = \frac{n_\alpha}{\sqrt{n_\alpha^2 - 1}} \left| \eta \cosh^{-1} \sqrt{\frac{n_\alpha^2 - t^2}{1 - t^2}} - \frac{1}{2} \eta \log_e \frac{\sqrt{n_\alpha^2 - t^2} + t \sqrt{n_\alpha^2 - 1}}{\sqrt{n_\alpha^2 - t^2} - t \sqrt{n_\alpha^2 - 1}} \right|_{t_{\alpha\beta}}^{t_{\alpha, N+1}} \quad (A6a)$$

$$t'_{\alpha\beta} = 1 \quad (t_{\alpha\beta} > 1; t_{\alpha\beta} < 0) \quad (A6b)$$

A special value of the function inside the brackets is given by

$$[] = \eta \log_e n_\alpha \quad (t = 1) \quad (A6c)$$

The formulas for τ are

$$\tau_{\alpha\beta} = \frac{n_\alpha}{\sqrt{1 - n_\alpha^2}} \frac{\pi |\eta|}{2} \left| \frac{t_{\alpha,N+1}}{t_{\alpha\beta}} \right| \quad (1 > t > n_\alpha) \quad (A7a)$$

$$t'_{\alpha\beta} = 1 \quad (t_{\alpha\beta} > 1; t_{\alpha\beta} < 0) \quad (A7b)$$

$$\begin{aligned} t'_{\alpha\beta} &= n_\alpha & (n_\alpha > t_{\alpha\beta} > 0) \\ t'_{\alpha,N+1} &= n_\alpha & (n_\alpha > t_{\alpha,N+1} > 0) \end{aligned} \quad \left. \right\} \quad (A7c)$$

and for v are

$$v_{\alpha\beta} = \frac{n_\alpha}{\sqrt{1 - n_\alpha^2}} \left| \frac{\pi \eta}{2} - \frac{\eta}{t} \sin^{-1} \sqrt{\frac{n_\alpha^2 - t^2}{1 - t^2}} - \eta \tan^{-1} \left(t \sqrt{\frac{1 - n_\alpha^2}{n_\alpha^2 - t^2}} \right) \right| \left| \frac{t_{\alpha,N+1}}{t_{\alpha\beta}} \right| \quad (1 > n_\alpha > t_{\alpha\beta} > 0) \quad (A8a)$$

$$t'_{\alpha\beta} = n_\alpha \quad (t_{\alpha\beta} > n_\alpha; t_{\alpha\beta} < 0) \quad (A8b)$$

The argument $t_{\alpha\beta}$ may be written

$$t_{\alpha\beta} = \frac{n_\alpha \eta}{n_\alpha - (1 - \eta)n_\beta} \quad (A9)$$

The argument n_α is given by

$$Bmn_\alpha = \frac{N - \alpha + 1}{N} \quad (A10)$$

Arrow Wing

An arrow wing is formed if the point on the root chord which lies at a distance $1 - \mu$ from the apex is joined by straight lines to the wing tips of the delta wing of figure 10 and the V-shaped segment formed is taken as a new trailing edge. If on the new root chord of length $(1 - \mu)$, N equal divisions are marked, a polygonal airfoil may be constructed as was done on the delta-wing root chord. The c_{cd} of this new wing may be calculated with the delta-wing formulas if minor substitutions are made as follows. In formula (A1) the limit N must be increased to $N + 1$. The corresponding additional $\Delta\lambda$ value, $\Delta\lambda_{N+1}$ is obtained from condition (A3a). The only other change is the substitution of the value $N' = \frac{N}{1 - \mu}$ for N , where N appears in the formulas (A4), (A6), (A7), (A8), and (A10). In formulas (A4), however, the substitution should not be made in the inequality $p, a, b \leq N$. In this inequality N becomes $N + 1$. The quantities c , c_{cd} , and t_r are, of course, all arrow-wing values.

Root Section ($\eta = 0$)

In the case of the root section the formulas for $t_{\alpha\beta}$, ρ , σ , τ , become somewhat simpler in form than those of the general case. The relations are

$$\frac{\eta}{t_{\alpha\beta}} = \frac{n_\alpha - n_\beta}{n_\alpha}$$

$$\rho_{\alpha\beta} = \tau_{\alpha\beta} = 0$$

$$\sigma_{\alpha\beta} = \frac{n_\alpha}{\sqrt{n_\alpha^2 - 1}} \cosh^{-1} n_\alpha \quad (\alpha \geq \beta)$$

$$\sigma_{\alpha\beta} = \frac{n_\beta}{\sqrt{n_\alpha^2 - 1}} \cosh^{-1} n_\alpha \quad (\alpha < \beta)$$

$$v_{\alpha\beta} = \frac{n_\alpha}{\sqrt{1 - n_\alpha^2}} \left(\frac{\pi}{2} - \sin^{-1} n_\alpha \right) \quad (\alpha \geq \beta)$$

$$v_{\alpha\beta} = \frac{n_\beta}{\sqrt{1 - n_\alpha^2}} \left(\frac{\pi}{2} - \sin^{-1} n_\alpha \right) \quad (\alpha < \beta)$$

(All)

Tip Section ($\eta = 1$)

At the tip section the ρ , σ , and τ functions and the v summations vanish; these conditions indicate that $cc_d = 0$. In order to evaluate the limit of c_d at the tip the limiting values of $\frac{1}{c}$ times ρ , σ , and τ must be calculated. For $\frac{\rho}{c}$ and $\frac{\sigma}{c}$ the limit is complicated by the fact that the subsonic ridge lines, along which the pressure has an infinite discontinuity, intersect at the tip. A finite limit in this case is preserved by the sharp trailing-edge condition (eq. (A3b)). The limit at the tip may be evaluated by expanding equations (A5a) and (A6a) for ρ and σ in a power series about $t = 1$ and taking the limit in equation (A1) as c goes to zero. The resulting limit may be written as

$$\frac{\pi}{8m} \left\{ \frac{c_{d, \text{tip}}}{t_r^2} \right\} = \frac{1}{2} \sum_{\alpha=1}^p \sum_{\beta=1}^{N+1} \frac{n_\alpha - n_\beta}{\sqrt{n_\alpha^2 - 1}} \log_e |\beta - \alpha| \Delta \lambda_\alpha \Delta \lambda_\beta + \sum_{\alpha=p+1}^{N+1} \sum_{\beta=1}^{N+1} \frac{\tau_{\alpha\beta}}{c} \Delta \lambda_\alpha \Delta \lambda_\beta \quad (\text{A12})$$

where the values of $\frac{\tau_{\alpha\beta}}{c}$ are given by

$$\left. \begin{aligned} \frac{\tau_{\alpha\beta}}{c} &= \frac{n_\alpha}{\sqrt{1 - n_\alpha^2}} \frac{\pi}{2} & (\alpha \geq \beta) \\ \frac{\tau_{\alpha\beta}}{c} &= \frac{n_\beta}{\sqrt{1 - n_\alpha^2}} \frac{\pi}{2} & (\beta > \alpha) \end{aligned} \right\} \quad (\text{A13})$$

as c goes to zero.

REFERENCES

1. Jones, Robert T.: Thin Oblique Airfoils at Supersonic Speed. NACA Rep. 851, 1946. (Supersedes NACA TN 1107.)
2. Ferri, Antonio: Elements of Aerodynamics of Supersonic Flows. The MacMillan Co., 1949.
3. Lighthill, M. J.: Supersonic Flow Past Bodies of Revolution. R. & M. No. 2003, British A.R.C., 1945.
4. Loftin, Laurence K., Jr.: Theoretical and Experimental Data for a Number of NACA 6A-Series Airfoil Sections. NACA Rep. 903, 1948. (Supersedes NACA TN 1368.)
5. Van Dyke, Milton D.: Subsonic Edges in Thin-Wing and Slender-Body Theory. NACA TN 3343, 1954.
6. Cooper, Morton, and Grant, Frederick C.: Minimum-Wave-Drag Airfoil Sections for Arrow Wings. NACA TN 3183, 1954.
7. Cooper, Morton, Smith, Norman F., and Kainer, Julian H.: A Pressure-Distribution Investigation of a Supersonic Aircraft Fuselage and Calibration of the Mach Number 1.59 Nozzle of the Langley 4- by 4-Foot Supersonic Tunnel. NACA RM L9E27a, 1949.
8. Harder, Keith C., and Rennemann, Conrad, Jr.: On Boattail Bodies of Revolution Having Minimum Wave Drag. NACA Rep. 1271, 1956. (Supersedes NACA TN 3478.)
9. Beane, Beverly: The Characteristics of Supersonic Wings Having Biconvex Sections. Jour. Aero. Sci., vol. 18, no. 1, Jan. 1951, pp. 7-20.

TABLE II.- PRESSURE COEFFICIENTS ON 65A WING - Continued

(c) Reynolds number = 4.3×10^6 ; free transition

X/C	ANGLE OF ATTACK, α														X/C	
	0		2		4		6		8		10		14			
	U	L	U	L	U	L	U	L	U	L	U	L	U	L		
$2y/b = 0.10$																
.000	.416		.377	.443	.329	.468	.279	.488	.199	.472	.116	.472	.035	.416	.000	
.024	.095		.052	.148	-.011	.199	-.069	.252	-.131	.300	-.191	.350	-.315	.448	.024	
.072	.081		.043	.108	.003	.155	-.034	.193	-.080	.235	-.131	.285	-.222	.387	.072	
.098	.069		.037	.094	.000	.141	-.033	.180	-.062	.220	-.089	.269	-.159	.367	.098	
.122	.067		.035	.097	.000	.137	-.026	.182	-.051	.219	-.078	.270	-.189	.336	.122	
.147	.056		.027	.086	-.007	.125	-.031	.166	-.057	.202	-.086	.248	-.139	.339	.147	
.172	.051		.023	.072	-.010	.111	-.035	.153	-.063	.190	-.091	.228	-.140	.318	.172	
.197	.047		.022	.071	-.014	.106	-.038	.144	-.065	.180	-.091	.221	-.140	.322	.197	
.246	.046		.009	.069	-.023	.105	-.045	.140	-.071	.178	-.095	.216	-.139	.295	.246	
.274	.040		.014	.057	-.018	.093	-.044	.131	-.072	.169	-.100	.213	-.145	.304	.274	
.300	.017		.017	.058	-.011	.091	-.034	.129	-.056	.165	-.081	.220	-.129	.312	.300	
.324	-.007		.005	.066	-.016	.100	-.035	.142	-.059	.184	-.080	.232	-.127	.316	.324	
.349	-.011		-.030	.049	-.056	.089	-.072	.126	-.092	.158	-.112	.179	-.144	.348	.349	
.373	.004		.052	.024	-.088	.067	-.110	.103	-.123	.132	-.149	.164	-.177	.253	.373	
.399	.004		.046	.018	-.080	.054	-.102	.091	-.129	.126	-.161	.164	-.205	.255	.399	
.424	-.006		.041	.012	-.074	.044	-.098	.080	-.122	.113	-.145	.155	-.185	.237	.424	
.449	-.001		.030	.026	-.062	.058	-.086	.094	-.110	.128	-.134	.164	-.177	.251	.449	
.473	-.013		.039	.018	-.069	.050	-.091	.087	-.115	.119	-.138	.160	-.180	.245	.473	
.498	-.028		.053	.001	-.082	.031	-.103	.067	-.126	.099	-.147	.138	-.187	.220	.498	
.523	-.040		.064	-.011	-.092	.022	-.112	.055	-.135	.086	-.156	.124	-.193	.206	.523	
.549	-.044		.068	-.019	-.098	.010	-.115	.045	-.139	.076	-.161	.115	-.198	.199	.549	
.574	-.040		.065	-.014	-.094	.016	-.114	.051	-.137	.082	-.161	.120	-.200	.206	.574	
.598	-.041		.064	-.016	-.092	.015	-.114	.049	-.138	.082	-.160	.118	-.201	.203	.598	
.623	-.053		.075	-.028	-.102	.004	-.122	.038	-.144	.070	-.164	.105	-.205	.188	.623	
.649	-.058		.081	-.036	-.107	-.006	-.127	.027	-.149	.058	-.169	.091	-.206	.179	.649	
.674	-.066		.089	-.043	-.115	-.012	-.133	.020	-.154	.051	-.173	.088	-.211	.177	.674	
.724	-.078		.098	-.054	-.126	-.026	-.143	.007	-.162	.035	-.182	.071	-.217	.166	.724	
.749	-.083		.103	-.060	-.129	-.033	-.146	-.002	-.165	.027	-.184	.061	-.219	.156	.749	
.772	-.078		.098	-.056	-.124	-.032	-.140	-.003	-.165	.024	-.178	.060	-.212	.163	.772	
.798	-.079		.097	-.059	-.121	-.033	-.137	-.002	-.156	.027	-.174	.063	-.208	.169	.798	
.824	-.077		.093	-.055	-.118	-.029	-.133	-.002	-.153	.032	-.170	.068	-.204	.174	.824	
.848	-.076		.093	-.055	-.117	-.029	-.135	-.004	-.155	.033	-.172	.069	-.205	.177	.848	
.874	-.079		.097	-.056	-.121	-.029	-.138	-.004	-.159	.034	-.177	.070	-.213	.179	.874	
.898	-.071		.090	-.051	-.116	-.024	-.132	-.009	-.154	.039	-.173	.075	-.209	.184	.898	
.923	-.073		.092	-.051	-.119	-.023	-.137	-.009	-.158	.040	-.177	.077	-.212	.183	.923	
.950	-.072		.092	-.051	-.119	-.023	-.136	-.010	-.159	.040	-.178	.076	-.215	.186	.950	
.974	-.069		.091	-.048	-.118	-.020	-.136	-.013	-.158	.044	-.178	.081	-.214	.189	.974	
$2y/b = 0.25$																
.000	.307		.336	.253	.338	.166	.323	.074	.302	-.002	.277	-.073	.243	-.215	.000	
.023	.074		.005	.135	-.115	.200	-.203	.260	-.271	.310	-.336	.357	-.424	.457	.023	
.048	.049		.011	.099	-.094	.159	-.170	.215	-.247	.264	-.315	.315	-.404	.415	.048	
.072	.042		.009	.087	-.076	.138	-.156	.190	-.248	.238	-.320	.285	-.412	.380	.072	
.098	.039		.006	.079	-.060	.127	-.117	.177	-.213	.223	-.310	.269	-.401	.372	.098	
.123	.033		.009	.068	-.054	.112	-.090	.161	-.158	.206	-.285	.258	-.359	.355	.123	
.148	.025		.015	.059	-.060	.104	-.086	.151	-.121	.197	-.215	.243	-.338	.342	.148	
.173	.023		.015	.050	-.049	.093	-.086	.164	-.118	.196	-.144	.245	-.316	.330	.173	
.199	.020		.021	.047	-.064	.091	-.091	.140	-.123	.176	-.148	.216	-.310	.310	.199	
.222	.016		.019	.049	-.060	.093	-.088	.133	-.119	.172	-.143	.220	-.307	.312	.222	
.248	-.007		.032	.022	-.072	.062	-.099	.102	-.130	.146	-.158	.197	-.310	.295	.248	
.273	.004		.027	.028	-.067	.070	-.095	.113	-.124	.159	-.148	.213	-.302	.297	.273	
.298	-.002		.025	.037	-.062	.072	-.090	.120	-.117	.144	-.142	.207	-.295	.285	.298	
.323	-.026		.035	.023	-.062	.040	-.089	.102	-.115	.140	-.142	.171	-.285	.291	.323	
.348	-.037		.046	.014	-.070	.049	-.097	.088	-.119	.117	-.142	.149	-.277	.242	.348	
.372	-.036		.058	.005	-.084	.040	-.106	.074	-.126	.110	-.147	.151	-.269	.243	.372	
.424	-.031		.079	-.012	-.114	.027	-.136	.067	-.157	.104	-.179	.147	-.245	.234	.424	
.449	-.035		.075	-.016	-.116	.022	-.145	.060	-.171	.097	-.194	.140	-.227	.225	.449	
.475	-.046		.078	-.022	-.115	.012	-.142	.051	-.178	.087	-.198	.127	-.224	.211	.475	
.500	-.053		.082	-.027	-.116	.008	-.142	.044	-.169	.079	-.196	.119	-.220	.202	.500	
.523	-.058		.084	-.029	-.116	.003	-.142	.039	-.168	.074	-.193	.113	-.214	.195	.523	
.549	-.066		.092	-.038	-.124	-.006	-.146	.029	-.171	.064	-.195	.104	-.216	.188	.549	
.573	-.066		.093	-.039	-.124	-.007	-.148	.029	-.172	.062	-.194	.102	-.217	.194	.573	
.598	-.070		.096	-.043	-.127	-.010	-.149	.024	-.173	.062	-.195	.103	-.222	.194	.598	
.624	-.071		.097	-.045	-.129	-.012	-.151	.023	-.175	.059	-.198	.099	-.228	.193	.624	
.648	-.074		.100	-.049	-.131	-.018	-.153	.018	-.178	.053	-.201	.082	-.231	.186	.648	
.674	-.075		.100	-.051	-.131	-.021	-.153	.015	-.177	.050	-.200	.086	-.233	.181	.674	
.699	-.079		.104	-.056	-.133	-.025	-.154	.009	-.177	.041	-.199	.078	-.233	.177	.699	
.723	-.082		.106	-.060	-.135	-.030	-.154	.004	-.179	.036	-.201	.075	-.233	.175	.723	
.749	-.088		.111	-.064	-.139	-.036	-.159	-.002	-.180	.031	-.202	.068	-.233	.170	.749	
.798	-.092		.115	-.069	-.142	-.040	-.161	-.007	-.182	.025	-.202	.062	-.231	.171	.798	
.848	-.094		.115	-.072	-.142	-.043	-.161	-.010	-.181	.022	-.200	.060	-.233	.174	.848	
.899	-.090		.111	-.069	-.138	-.041	-.158	-.007	-.177	.026	-.197	.063	-.231	.172	.899	
.948	-.086		.106	-.068	-.133	-.036	-.153	-.002	-.173	.031	-.196	.070	-.225	.178	.948	

TABLE II.- PRESSURE COEFFICIENTS ON 65A WING - Continued

(c) Concluded

X/C	ANGLE OF ATTACK, α														X/C	
	0		2		4		6		8		10		14			
	U	L	U	L	U	L	U	L	U	L	U	L	U	L		
$2y/b = 0.40$																
.000	.308		.341	.303	.259	.225	.190	.089	.099	.011	.008	.089	.140	.211	.000	
.026	.053		.045	.122	.179	.195	.261	.256	.335	.302	.397	.343	.461	.412	.026	
.048	.033		.049	.093	.173	.159	.269	.219	.335	.268	.389	.321	.450	.406	.048	
.075	.025		.041	.080	.145	.142	.248	.200	.319	.253	.377	.305	.454	.399	.075	
.100	.016		.043	.065	.133	.123	.244	.180	.319	.234	.378	.277	.458	.379	.100	
.125	.014		.038	.057	.111	.112	.226	.171	.313	.213	.372	.261	.449	.365	.125	
.145	.009		.040	.051	.106	.106	.211	.159	.310	.203	.371	.255	.445	.359	.145	
.199	.003		.043	.040	.085	.083	.118	.143	.284	.194	.361	.250	.419	.330	.199	
.248	.002		.047	.032	.095	.084	.125	.131	.148	.186	.335	.225	.368	.302	.248	
.298	.014		.048	.029	.092	.078	.127	.123	.151	.162	.221	.196	.354	.288	.298	
.350	.035		.052	.019	.090	.053	.127	.091	.152	.130	.175	.175	.350	.267	.350	
.401	.038		.059	.004	.089	.040	.119	.080	.145	.123	.169	.149	.348	.253	.401	
.426	.055		.083	.019	.115	.020	.136	.062	.157	.102	.182	.146	.355	.233	.426	
.450	.060		.098	.032	.126	.009	.146	.051	.168	.091	.191	.134	.358	.219	.450	
.475	.063		.110	.036	.141	.001	.160	.040	.180	.082	.198	.122	.360	.208	.475	
.500	.068		.114	.040	.149	.002	.168	.038	.187	.079	.207	.118	.365	.207	.500	
.526	.070		.113	.042	.156	.007	.177	.030	.196	.069	.214	.109	.366	.201	.526	
.550	.080		.113	.052	.159	.014	.186	.024	.208	.063	.224	.104	.368	.200	.550	
.575	.085		.116	.056	.159	.020	.190	.018	.214	.053	.231	.095	.367	.195	.575	
.600	.091		.120	.063	.159	.030	.191	.009	.217	.045	.235	.087	.370	.190	.600	
.629	.089		.117	.059	.152	.025	.181	.014	.211	.051	.229	.093	.370	.199	.629	
.650	.093		.120	.067	.157	.031	.182	.008	.211	.046	.231	.089	.372	.196	.650	
.674	.103		.129	.076	.165	.042	.187	.003	.217	.035	.241	.074	.375	.184	.674	
.699	.106		.131	.079	.165	.043	.189	.005	.215	.032	.238	.072	.372	.180	.699	
.724	.106		.133	.079	.165	.044	.188	.005	.213	.031	.237	.071	.369	.177	.724	
.750	.106		.132	.078	.166	.042	.189	.006	.213	.029	.237	.067	.364	.180	.750	
.799	.102		.128	.075	.162	.042	.186	.008	.208	.024	.232	.060	.355	.167	.799	
.850	.102		.126	.078	.160	.046	.184	.013	.206	.021	.228	.060	.346	.172	.850	
.899	.103		.125	.079	.157	.046	.180	.013	.201	.020	.222	.056	.338	.165	.899	
.950	.101		.125	.080	.156	.048	.179	.017	.198	.020	.219	.058	.318	.166	.950	
$2y/b = 0.60$																
.000	.297		.262	.276	.104	.225	.071	.159	.181	.077	.259	.001	.373	.088	.000	
.023	.071		.052	.162	.193	.237	.284	.288	.390	.328	.452	.360	.479	.417	.023	
.046	.022		.095	.108	.244	.196	.313	.253	.394	.305	.448	.346	.475	.425	.046	
.076	.004		.099	.080	.250	.193	.324	.219	.389	.273	.456	.314	.473	.407	.076	
.100	.002		.088	.069	.238	.137	.320	.195	.379	.250	.429	.290	.473	.386	.100	
.122	.007		.075	.062	.225	.132	.313	.188	.373	.238	.428	.278	.474	.379	.122	
.149	.005		.078	.066	.211	.123	.306	.173	.369	.222	.422	.259	.475	.362	.149	
.200	.011		.083	.029	.193	.098	.297	.152	.365	.194	.416	.242	.473	.341	.200	
.249	.028		.086	.023	.176	.081	.294	.126	.363	.171	.412	.222	.470	.317	.249	
.299	.040		.092	.008	.154	.067	.287	.113	.364	.152	.412	.203	.466	.294	.299	
.348	.051		.097	.002	.149	.052	.277	.094	.361	.135	.413	.179	.441	.276	.348	
.400	.048		.101	.014	.150	.028	.235	.068	.354	.111	.414	.157	.452	.255	.400	
.424	.073		.100	.018	.152	.022	.188	.063	.351	.106	.413	.149	.448	.255	.424	
.448	.085		.110	.033	.157	.003	.173	.048	.350	.093	.414	.135	.446	.243	.448	
.473	.088		.113	.039	.157	.001	.182	.049	.346	.089	.411	.133	.441	.241	.473	
.498	.093		.117	.052	.160	.007	.188	.034	.343	.079	.410	.124	.437	.231	.498	
.525	.102		.125	.062	.162	.018	.191	.028	.341	.071	.409	.114	.437	.224	.525	
.553	.115		.145	.077	.175	.035	.200	.009	.339	.051	.410	.092	.437	.204	.553	
.575	.115		.151	.083	.179	.038	.202	.007	.330	.048	.408	.092	.436	.203	.575	
.600	.115		.153	.081	.183	.038	.204	.008	.302	.051	.401	.092	.434	.207	.600	
.650	.122		.166	.089	.197	.049	.211	.004	.225	.035	.392	.076	.431	.194	.650	
.703	.127		.178	.096	.208	.056	.222	.016	.218	.023	.370	.064	.427	.186	.703	
.751	.131		.174	.098	.215	.061	.229	.020	.228	.019	.332	.064	.422	.180	.751	
.798	.134		.170	.100	.220	.064	.237	.023	.241	.018	.290	.060	.419	.180	.798	
.851	.128		.161	.096	.215	.060	.235	.016	.240	.024	.260	.067	.410	.182	.851	
$2y/b = 0.80$																
.000	.233		.084	.260	.188	.262	.346	.240	.423	.203	.470	.171	.470	.144	.000	
.069	.009		.166	.081	.304	.169	.390	.226	.450	.274	.482	.314	.457	.408	.069	
.120	.033		.168	.047	.310	.127	.386	.184	.441	.231	.476	.279	.454	.381	.120	
.169	.043		.158	.030	.308	.103	.380	.162	.435	.210	.472	.257	.454	.366	.169	
.219	.067		.159	.004	.304	.075	.375	.129	.432	.180	.468	.228	.452	.330	.219	
.270	.071		.156	.009	.299	.061	.370	.114	.428	.164	.466	.211	.453	.321	.270	
.321	.080		.161	.015	.297	.044	.366	.095	.425	.145	.463	.191	.450	.301	.221	
.373	.087		.162	.023	.297	.027	.364	.080	.421	.126	.463	.174	.446	.287	.373	
.421	.098		.164	.035	.297	.011	.365	.061	.419	.109	.460	.154	.444	.262	.421	
.469	.109		.171	.049	.297	.005	.367	.044	.420	.091	.459	.144	.442	.259	.469	
.520	.123		.175	.067	.298	.024	.371	.026	.421	.075	.460	.124	.437	.243	.520	
.574	.134		.182	.082	.300	.038	.375	.012	.424	.066	.459	.107	.429	.224	.574	
.622	.145		.191	.091	.299	.051	.376	.002	.425	.053	.458	.095	.424	.214	.622	
.673	.155		.199	.104	.298	.060	.377	.007	.424	.038	.457	.080	.418	.199	.673	
.724	.163		.198	.113	.296	.067	.378	.016	.424	.029	.457	.073	.415	.196	.724	
.774	.177		.201	.135	.289	.084	.380	.022	.422	.002	.455	.064	.415	.172	.774	
.824	.170		.200	.129	.273	.080	.377	.031	.417	.011	.455	.054	.409	.180	.824	
.872	.172		.199	.132	.259	.081	.375	.033	.409	.009	.453	.054	.406	.176	.872	

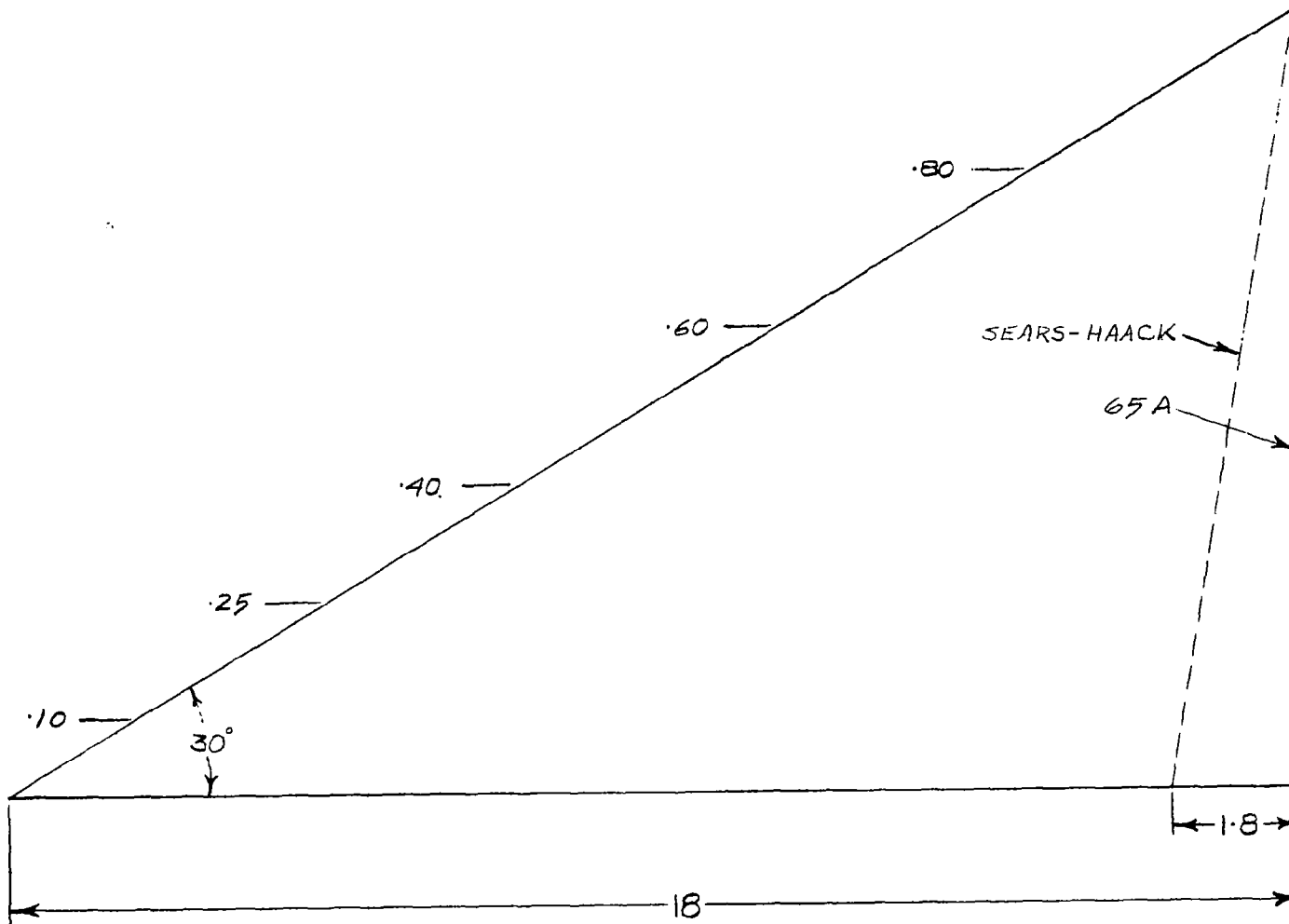


Figure 1.- Plan form of test wings.

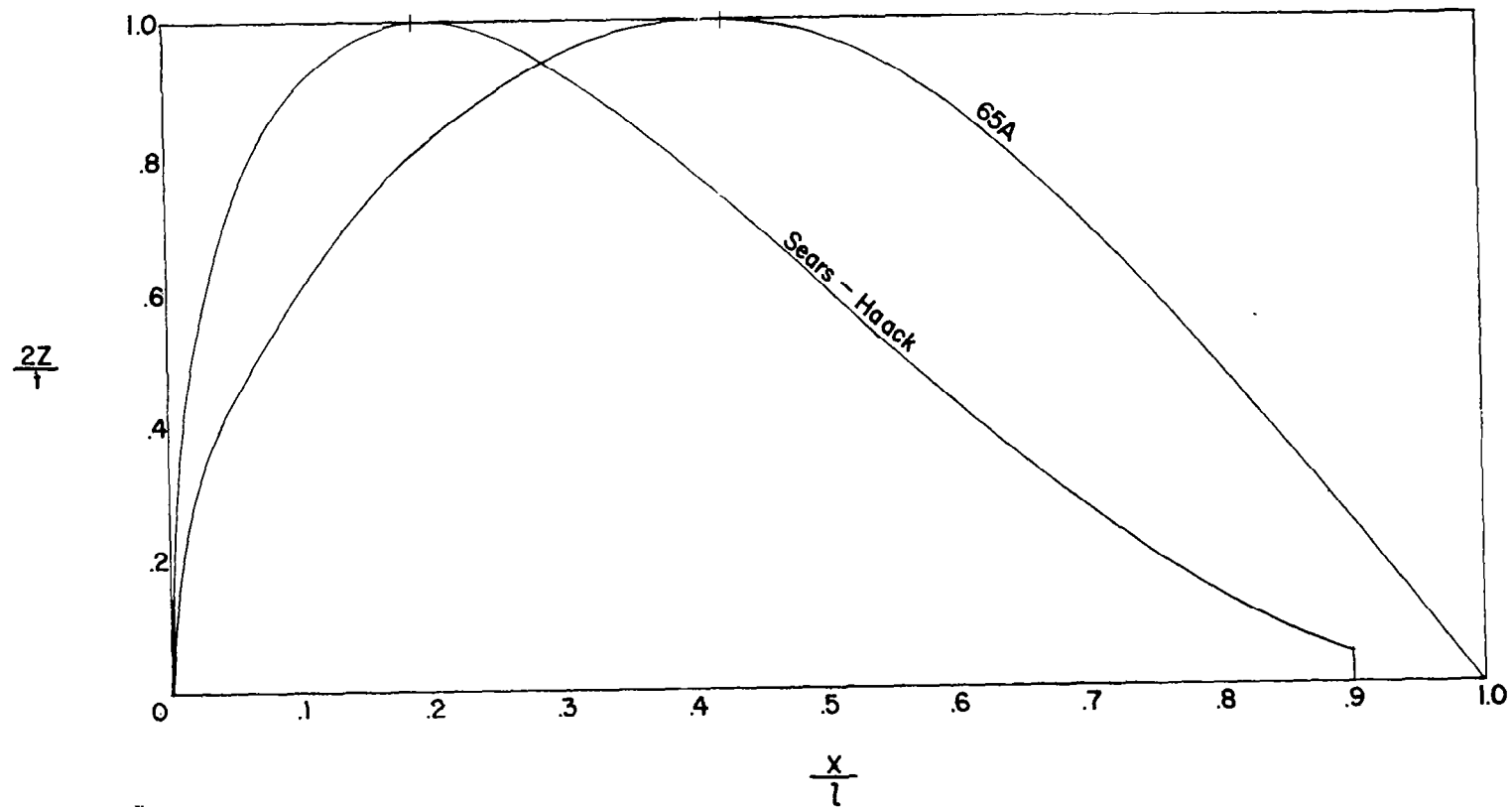


Figure 2.- Root sections of test models.

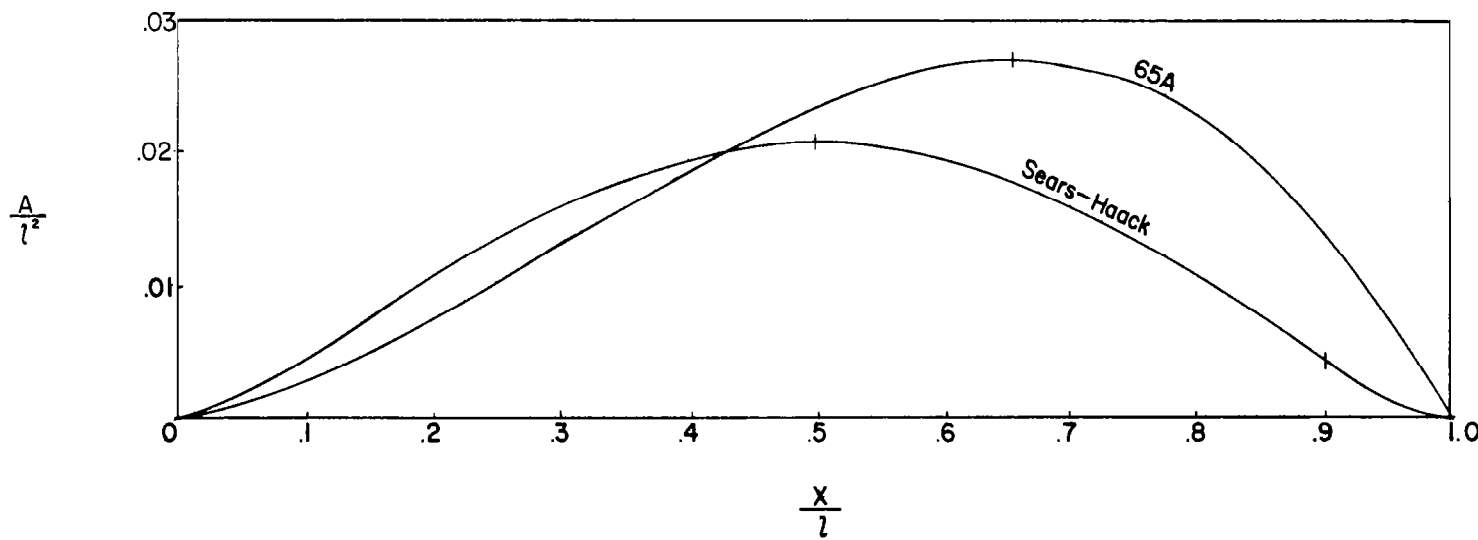


Figure 3.- Cross-sectional area distributions of test wings.

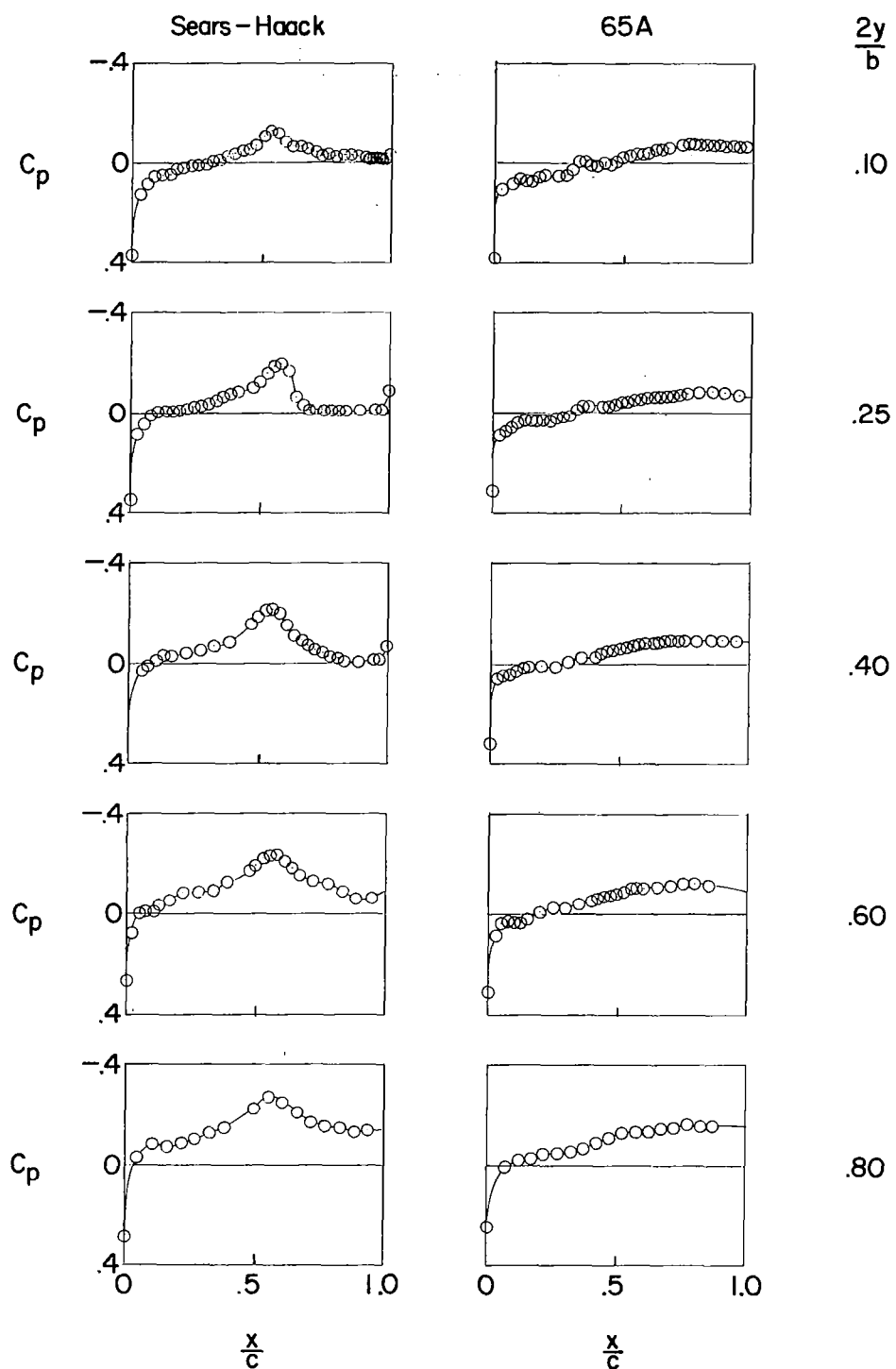


Figure 4.- Pressure distributions on streamwise direction. $\alpha = 0^\circ$.

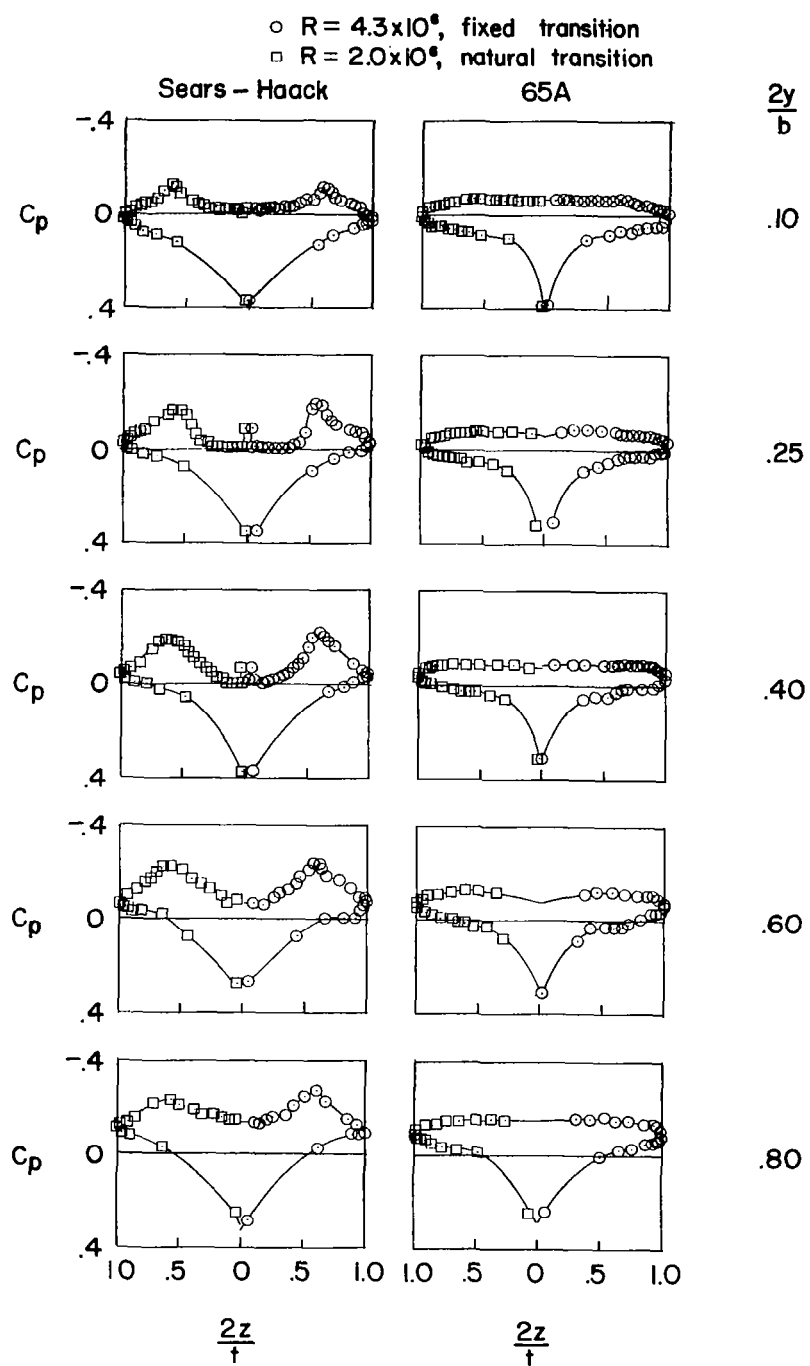


Figure 5.- Pressure distributions in normal direction. $\alpha = 0^\circ$.

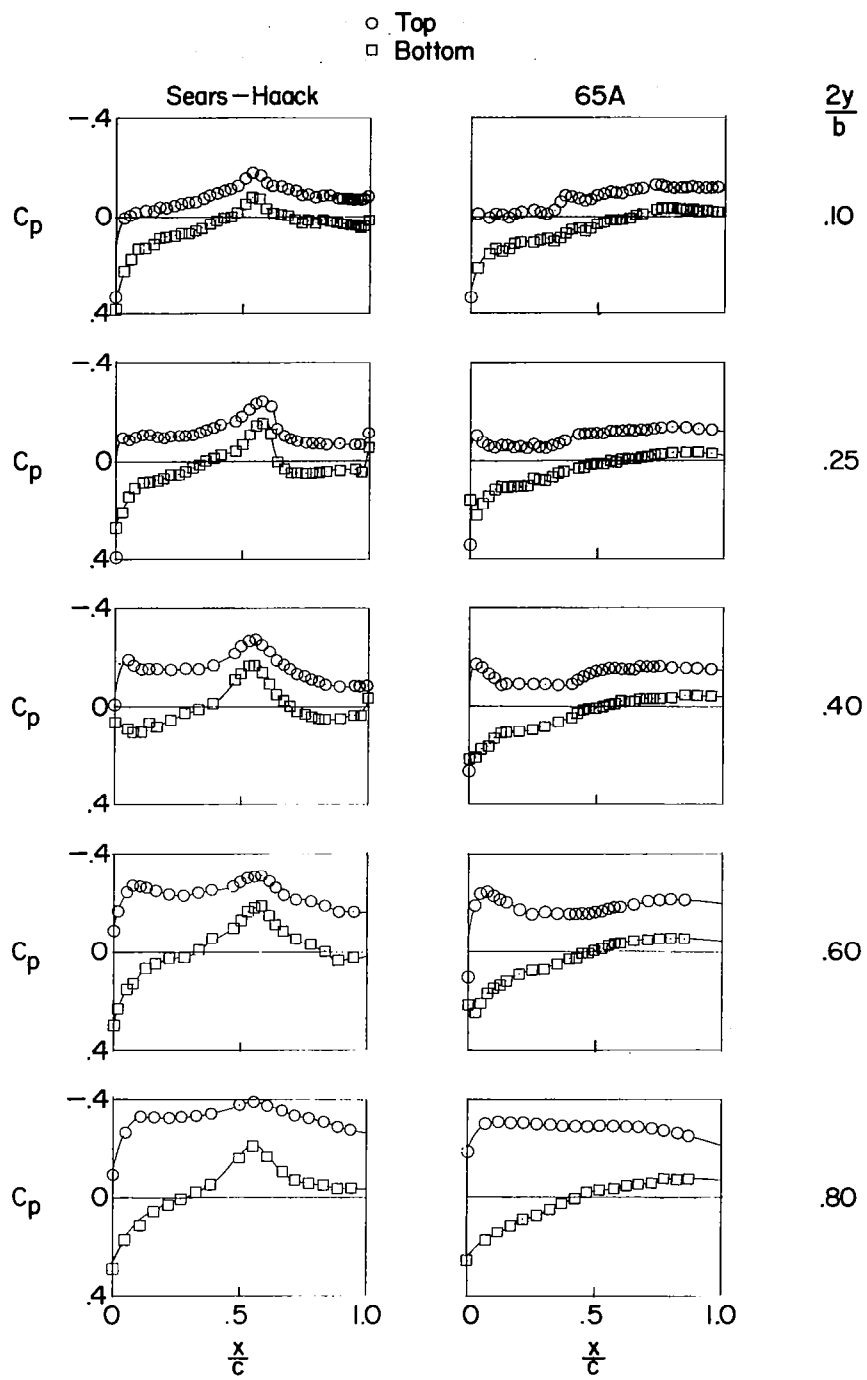
(a) $\alpha = 4^\circ$.

Figure 6.- Pressure distributions at positive lift.

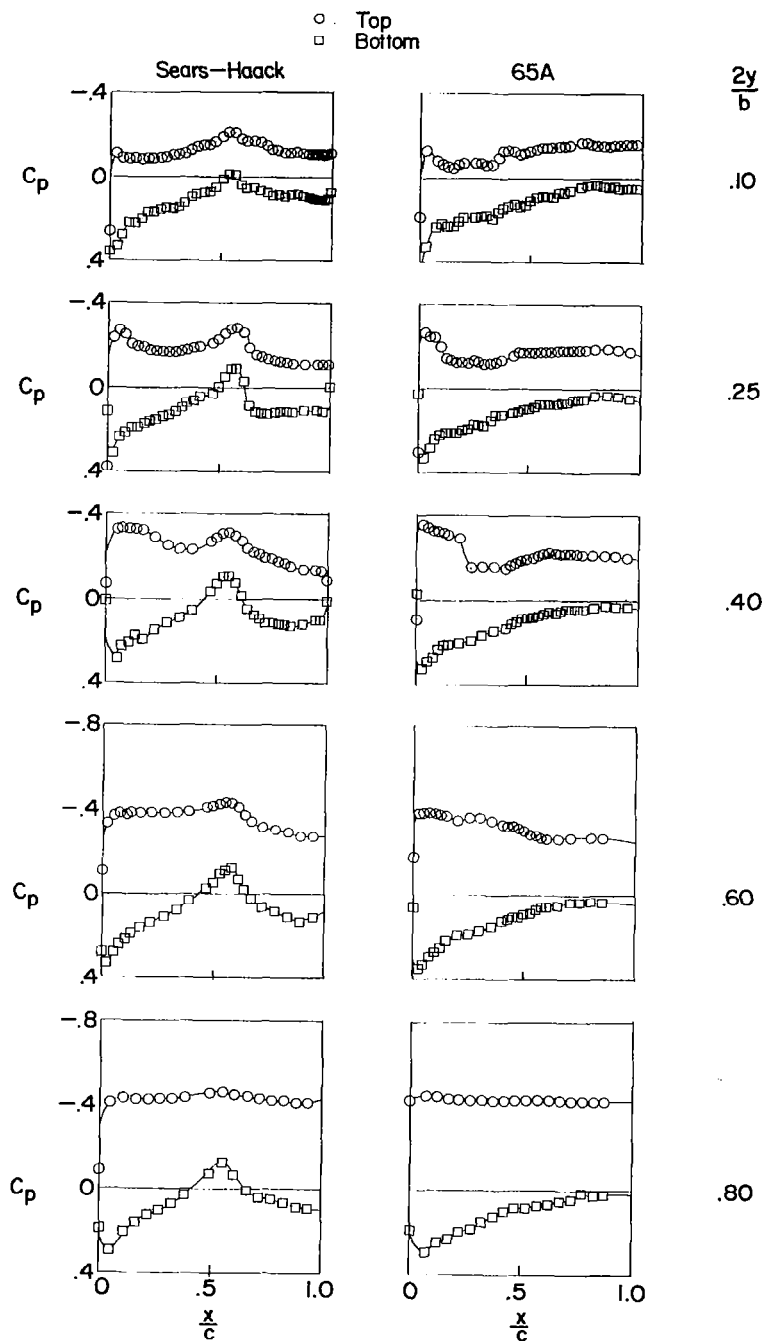
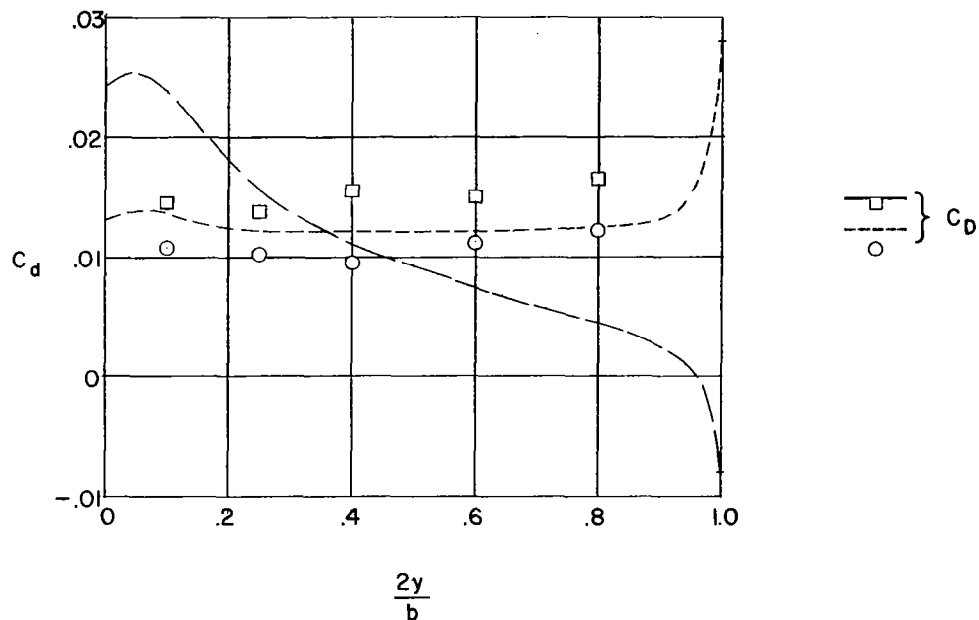
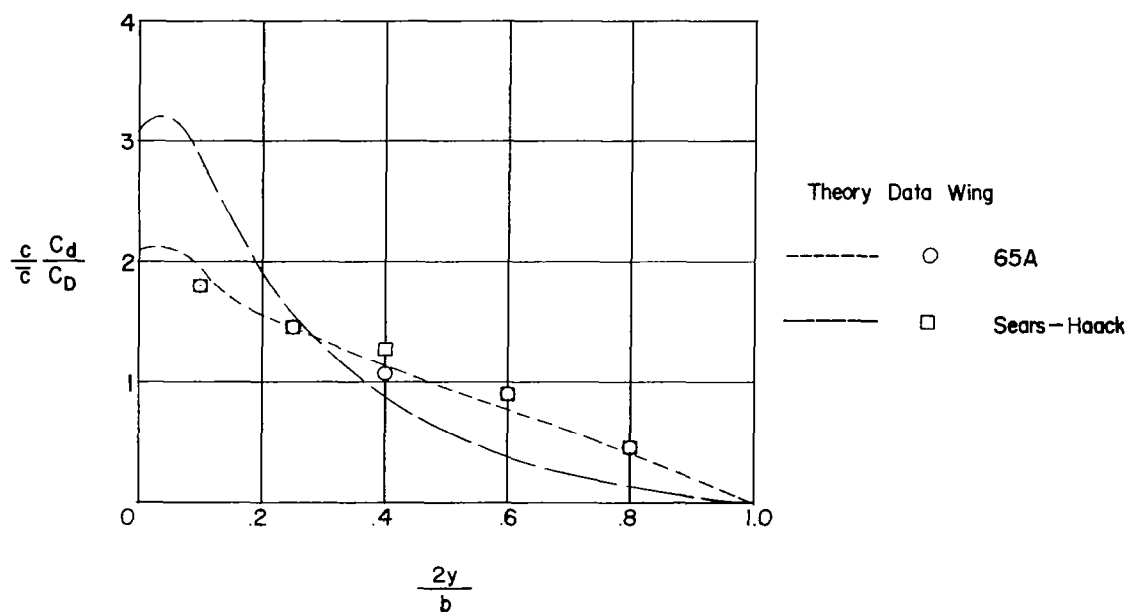
(b) $\alpha = 8^\circ$.

Figure 6.- Concluded.



(a) Spanwise drag distribution.



(b) Section wave drag coefficient.

Figure 7.- Experimental and theoretical drag values.

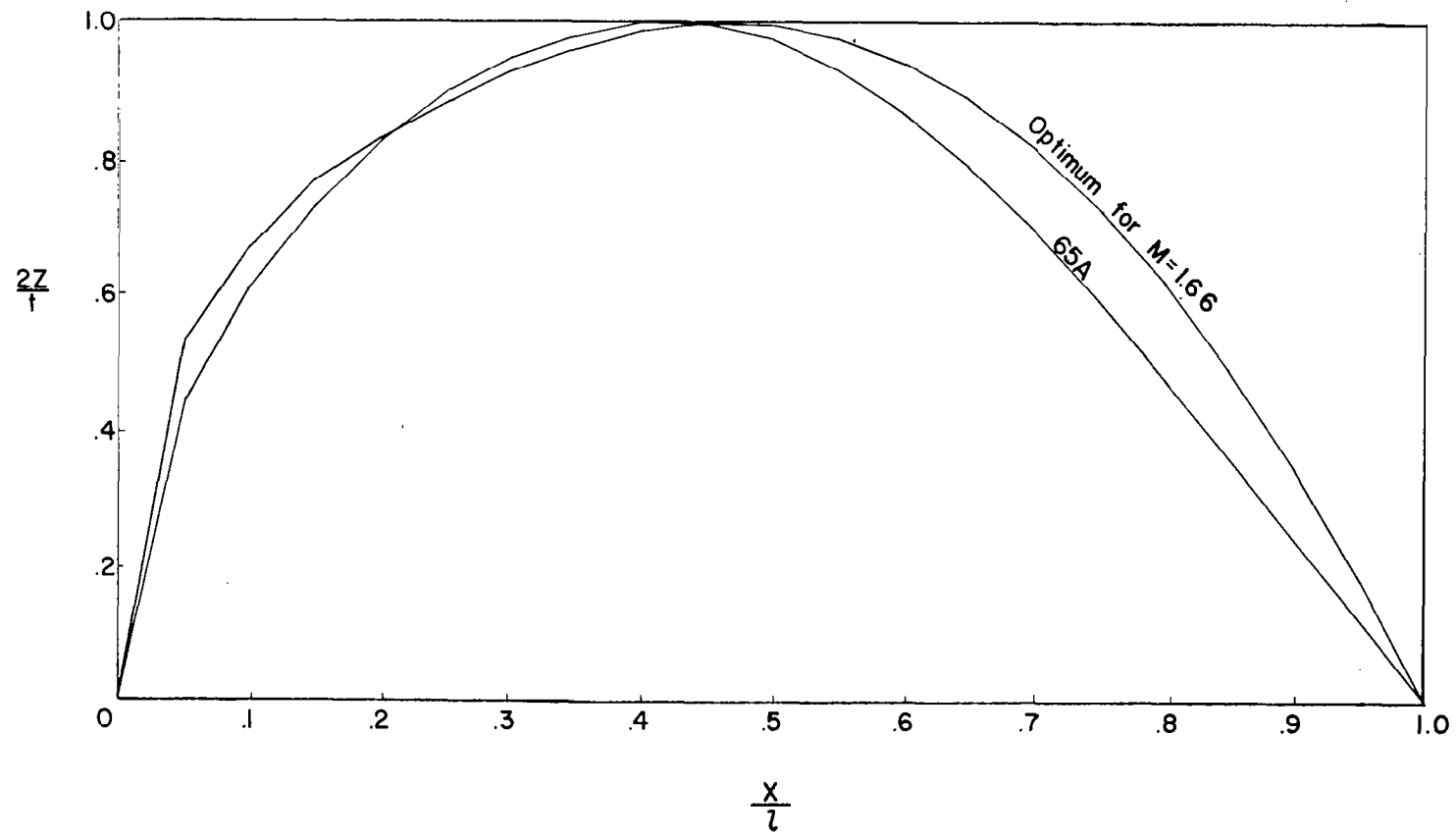
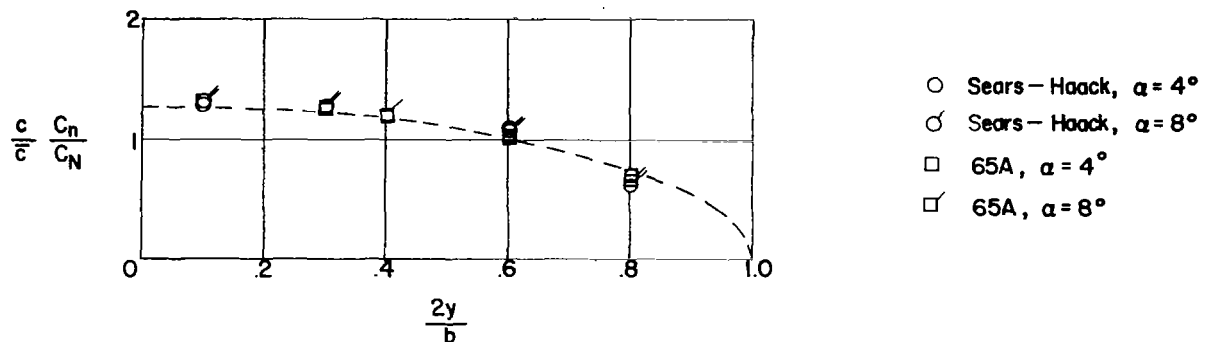
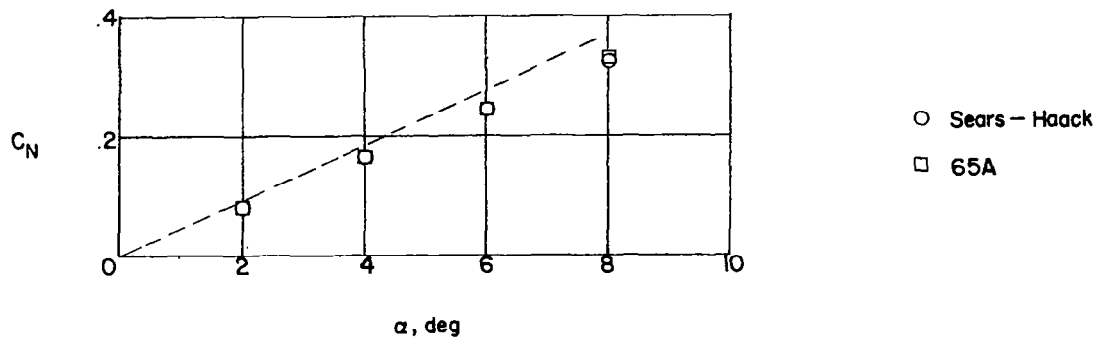


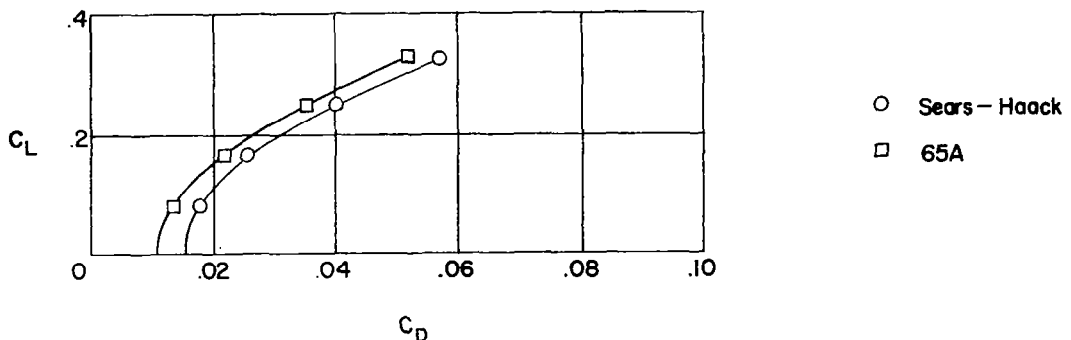
Figure 8.- Comparative thickness distributions. Polygonal airfoils with $N = 20$.



(a) Normalized normal-force landing along the span.



(b) Normal force and angle of attack.



(c) Pressure drag coefficient and lift coefficient.

Figure 9.- Variation of span loading and normal-force coefficient with angle of attack. Dotted lines indicate linear theory values for a delta wing.

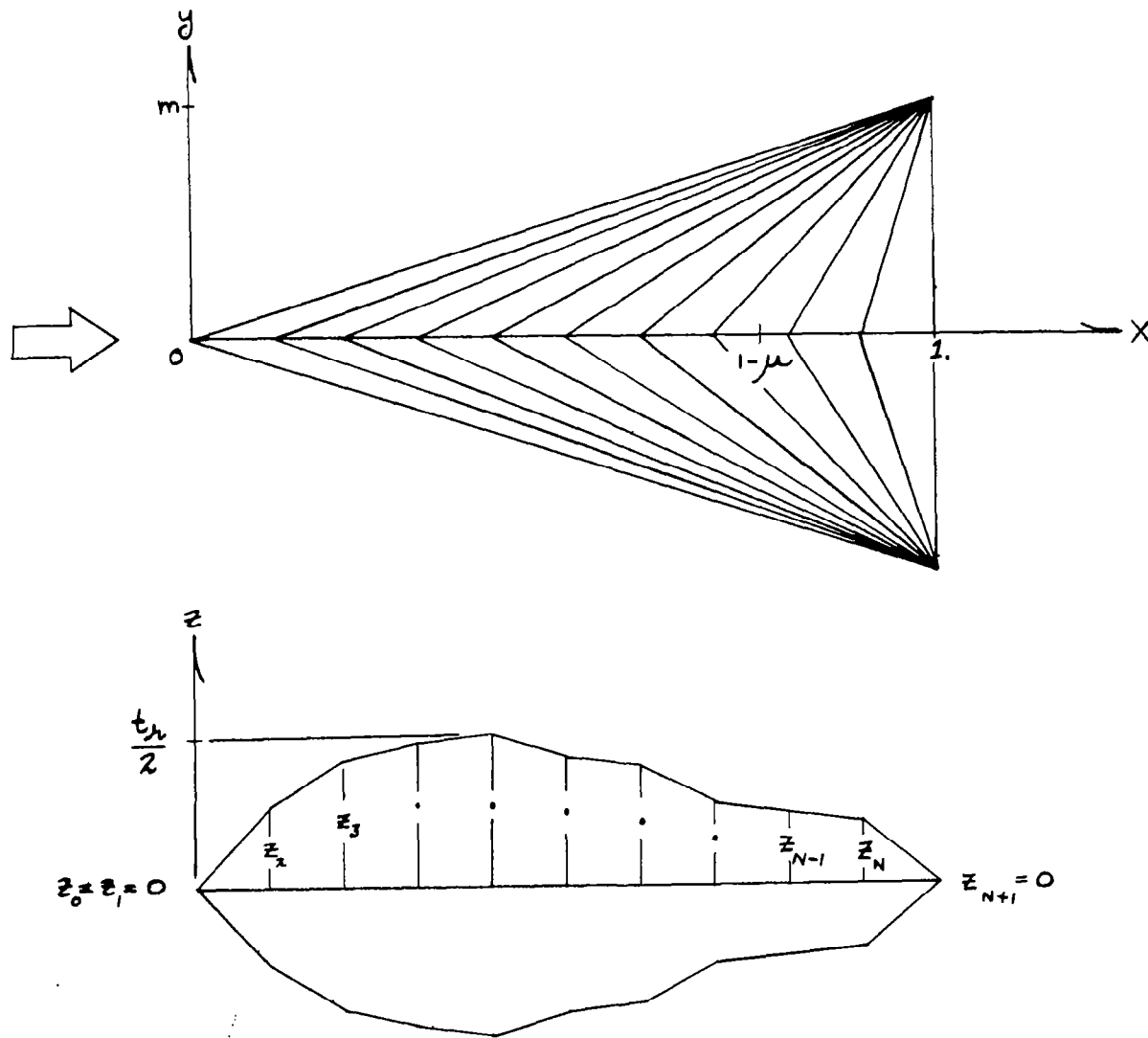


Figure 10.- Delta plan form and polygonal airfoil section.